THE ASTROPHYSICAL JOURNAL, 250:517–527, 1981 November 15

THE EXTENDED H I DISK OF THE S0 GALAXY NGC 4203

DAVID BURSTEIN
National Radio Astronomy Observatory,[1] Charlottesville, Virginia
AND
NATHAN KRUMM
Department of Astronomy, University of Michigan
Received 1981 March 26; accepted 1981 May 19

ABSTRACT

An Arecibo 21 cm H I map of this remarkable galaxy is presented. As judged by the usual classification criteria, NGC 4203 is a fairly typical S0 galaxy, although its disk-to-bulge ratio is at the high end of that observed for S0's. Unlike most S0's, NGC 4203 is embedded in an H I disk at least 38 h^{-1} kpc in diameter, over three times the Holmberg size. The velocity field of the H I is generally indicative of a rotating disk with a flat rotation curve, but it is distorted in a manner suggesting an oval distortion or a kinematical warp. The distribution of gas in the outer parts of the galaxy is observed to be asymmetric and is inferred to be asymmetric near the center of the galaxy by combining the H I data with an inner optical rotation curve kindly provided by V. C. Rubin. Intercomparison of the H I profiles bracketing the center with the center profile indicates the gas has a central, unresolved minimum.

The integrated parameters for NGC 4203 derived from the Arecibo data are in good agreement with those previously derived by Knapp *et al.*. The rotation velocity in the plane of the H I disk is 210 ± 40 km s^{-1}, giving a mass of $7 \pm 2 \times 10^{10}\ h^{-1}\ M_{\odot}$ interior to the Holmberg radius (quoted errors are from the one sigma uncertainty in the inclination of the disk). The mass-to-light ratio at the Holmberg radius is $15 \pm 5\ h\ M_{\odot}/L_{\odot}$, but it is $35 \pm 12\ h$ inside the furthest measured point on the rotation curve. At least 60% of the mass in NGC 4203 must lie outside the Holmberg radius.

The observed kinematic and gas distribution properties of the H I disk in NGC 4203 and, to a lesser extent, the H I ring in the elliptical galaxy NGC 4278 (Raimond *et al.*) are shown to be very similar to those of warped spiral galaxies, like NGC 2841. However, the average gas column density in the two early-type galaxies is an order of magnitude lower than that in typical spiral galaxies. Such a low density of gas could inhibit star formation. From the marked similarity between the H I distributions in NGC 4203 and NGC 4278 and those in spiral galaxies, it is suggested that the H I distributions in these two early-type galaxies have the same origin as the H I distributions in spirals; i.e., that the H I disk in NGC 4203 is *intrinsic* to the galaxy.

Subject headings: galaxies: individual — galaxies: internal motions — galaxies: structure — radio sources: 21 cm radiation

I. INTRODUCTION

It is now well known that relatively few S0 and elliptical galaxies contain sufficient neutral hydrogen to be detectable by even sensitive radio telescope surveys (e.g., Knapp, Kerr, and Williams 1978). Most of the early-type galaxies with detected H I are unusually blue in color (Balick, Faber, and Gallagher 1976), indicating that stars are forming from the gas.

However, a substantial fraction of H I-detected elliptical and S0 galaxies are as red in color as nondetected galaxies and show no evidence of star formation on standard large-scale classification plates taken in the photographic B band. Little is known about the distribution or source of the gas in these red galaxies, although the global properties of some have the double-horned signature of a rotating disk of gas (cf. Krumm and Salpeter 1979*c*). While understanding the distribution of gas in these galaxies is central to discovering the origin of this gas, the mapping of the H I in these galaxies is hampered by the relatively low column densities and the high rotation velocity widths found in early-type galaxies.

Recent maps of H I in ellipticals and S0's have been published by Knapp, Kerr, and Williams (1978) and

[1]The National Radio Astronomy Observatory is operated by Associated Universities, Inc., under contract with the National Science Foundation.

Hart, Davies, and Johnson (1980), but both studies are of relatively low signal-to-noise ratio. High quality Westerbork maps have been obtained for a few early-type galaxies including NGC 4203; most are still in various processing stages (e.g., Shostak, van Woerden, and Schwarz 1979), but one on NGC 4278 has been published (Raimond *et al.* 1981).

In this discussion of NGC 4203 we present the first in a series of high signal-to-noise ratio maps of early-type galaxies made with the 300 m Arecibo radio telescope. These data should be viewed as complementary to the Westerbork observations, since Arecibo is substantially more sensitive to the large-scale distribution of H I in galaxies.

NGC 4203 is an optically unremarkable face-on S0 galaxy. Basic information about it is listed in Table 1. While its color is red, a deep ultraviolet plate of NGC 4203 taken by P. C. van der Kruit with the 1.2 m Palomar Schmidt does show evidence of low surface brightness star formation. A standard blue plate (Fig. 1 [Pl. 18]) only weakly shows a small dust cloud (*arrow*) in an otherwise featureless disk. An Hα plate obtained by one of us (N.K.) with the McGraw-Hill 1.3 m telescope fails to show any H II regions, although a similar plate of a spiral at the same redshift, NGC 3359, clearly shows all the H II regions cataloged by Hodge (1969).

Photographic surface photometry by Burstein (1979*b*) shows that NGC 4203 has an exponential disk and a moderate-sized bulge. Burstein (1979*c*) found NGC 4203 to a have a disk-to-bulge ratio (D/B) of 2.0, at the high end of the limited range of D/B found for S0's. The 26.5 mag arcsec^{-2} isophotal diameter of NGC 4203 is 4.2, or 13.4 h^{-1} kpc (where $h = H_0/100$ km s^{-1} Mpc^{-1}).

Infrared photoelectric surface photometry in the J band (1.3 microns) has been carried out by Hohlfeld and Krumm (1981) with the 1.3 m Kitt Peak National Observatory telescope. The $B-J$ color of the disk is 4.0 ± 0.5 mag, and there is no evidence of a strong color gradient from the nucleus out to at least 1.5 in radius. The intermediate band photoelectric study of Burstein (1979*a*) also found no evidence of star formation in NGC 4203, although the contribution of light from a young stellar population at 10% or less in B cannot be ruled out.

NGC 4203 is a weak radio continuum source with an integrated flux of 11 ± 4 mJy at 11 cm (Dressel and Condon 1978). Krumm and Sramek (1981) have detected the nucleus at 6 cm with the Very Large Array of the National Radio Astronomy Observatory and found that the emission comes from an unresolved ($\leq 1''$) point source. The 6 cm flux of 9.0 ± 0.7 mJy implies a radio spectrum with $\alpha = 0.3\pm0.5$.

An H I integrated flux of 20 ± 5 Jy km s^{-1} was measured by Knapp *et al.* (1977) using the NRAO 43 m telescope. Bieging and Biermann (1977) measured only 7 ± 1 Jy km s^{-1} with the Arecibo telescope. The discrepancy in flux measurements arises because the H I distribution is strongly resolved by the Arecibo beam. In this paper we present a full map of the H I distribution of NGC 4203 made with the 4′ Arecibo beam. Since this is the first of several such maps to be presented, § II is a detailed description of the data taking and reduction systems and presents the velocity profile parameters from these data, while § III details the distributions of velocity and gas in the galaxy. In § IV we compare the gas distribution in NGC 4203 to those in a spiral and an elliptical, and in § V we discuss possible implications of these comparisons.

II. OBSERVATIONS

a) Data Taking and Reduction

The H I spectra were obtained during two runs on the Arecibo[2] 305 m radio telescope during 1979 January and

[2]The Arecibo Observatory is part of the National Astronomy and Ionosphere Center, which is operated by Cornell University under contract with the National Science Foundation.

TABLE 1

OPTICAL PARAMETERS OF NGC 4203

Parameter	Value	Reference[a]
Morphological type	SAB0$^-$	1
B_T	11.55 ± 0.09	1
Galactic extinction A_B	0.00	2
"Holmberg" diameter	4.2 ± 0.2	3
Inclination, i	$27°\pm5°$	3
Disk-to-bulge luminosity ratio	2.0 ± 0.2	3
Adopted distance	10.8 h^{-1} Mpc	($H_0 = 100\,h$)
Absolute magnitude	-18.62 ± 0.10	
Absolute luminosity	$4.4\pm0.4\times10^9\,L_\odot$	4
Absolute Holmberg diameter	$13.4\pm0.6\,h^{-1}$ kpc	

[a]REFERENCES.—(1) de Vaucouleurs, de Vaucouleurs, and Corwin 1976 (RC2). (2) Burstein and Heiles 1978 and unpublished. (3) Burstein 1979*b*. (4) Allen 1973 ($M_\odot = 5.48$).

TABLE 2

ARECIBO 21 cm DATA-TAKING SYSTEM, FLAT FEED

Point source response	6.5° K Jy^{-1}
rms pointing error	35″
Half-power beamwidth:	
Zenith angle = 14°	4.′14 ± 0.′04
Zenith angle = 20°	5.′0
Peak sidelobe amplitude	3%
Sidelobe ring radius	6′
Sidelobe azimuthal extent	< 180°
Receiver noise temperature	65 K
Passband	5 MHz
Channel spacing	19.5 kHz
Resolution	8 km s^{-1}
On-source integration time—typically	3 minutes
Noise level per channel	6 mJy
rms flux error	0.9 Jy km s^{-1}

1980 June with the 21 cm flat feed. The characteristics of the system are summarized in Table 2 and are discussed below.

Considerable effort was spent determining the pointing reliability, system response as a function of zenith angle and frequency, and telescope beamshape. Radio continuum point sources of known position and flux were selected from the list of Bridle *et al.* (1972) and were observed with the Observatory's data-taking program PEAK, which adjusts the telescope pointing until maximum response is obtained. PEAK then prints out the pointing error and the ratio of source response to that of the calibration noise diode, mounted in the top of the feed. Measurements were made over the whole range of zenith and azimuth angles, and at several frequencies between 1408 and 1418 MHz. In 1979 the mean pointing error was found to be 35″, with maximum deviations of about 1′. In 1980 it had improved by a factor of 2. The variation of system response with frequency and zenith angle was measured in order to determine the corrections to be applied during data reduction. The value of the noise diode (which is pulsed at one second intervals during spectral line observations to calibrate the flux scale) was checked daily against these radio sources and was found to be constant to better than 2%.

The beam shape of the flat feed was measured by letting a source drift through the field. The main beam is approximately Gaussian in shape. For zenith angles less than 14%, the full width at half-maximum is 4.′14 ± 0.′04. From 14° to 20° it rises slowly to 5.′0. There was a sidelobe arc of radius about 6′ and azimuthal extent less than 180°, as seen from the center of the main beam. It appeared as a leading sidelobe for sources south of zenith (i.e., declination < 19°), and as a trailing sidelobe for sources north of zenith. The peak amplitude, which did not vary with zenith angle, was about 3% of the main beam amplitude. We believe the sidelobe is caused by other line feeds mounted on the carriage house interfering with the illumination pattern. It is *not* a serious problem for these measurements, since the strongest signal in any profile is only about 70 mJy. Three percent of this is 2 mJy, only one-third of the typical noise fluctuations.

The receiver is a cooled, parametric amplifier with a noise temperature average of about 65 K. A 5 MHz bandpass was employed, centered on a frequency corresponding to $c\Delta\lambda/\lambda_0 = 1000$ km s^{-1} with respect to the Sun. The signal was accumulated in 252 channels of the Observatory's three-level autocorrelator, and then Fourier transformed.[3] The final spectra were Hanning smoothed, and a linear baseline was removed. The spacing between channels was 19.5 kHz with a resolution of 39 kHz, or about 8 km s^{-1}.

Observations were made in beam-switching mode: typically three minutes integration on the galaxy were followed by three minutes on a blank sky position, chosen in such a way that the same range of zenith and azimuth angles was tracked. Most profiles represent a single on-off pair. The observations were taken at night, so baselines were usually fairly stable.

A spectrum of the galaxy center was taken on five separate occasions to test measurement repeatability. The rms scatter in the integrated flux was found to be 0.9 Jy km s^{-1}. About one-third of this is attributable to white noise (about 6 mJy per channel). The rest presumably comes from pointing errors and small baseline instabilities.

b) The Data

Spectra for 55 locations in the galaxy were obtained. The observations covered a grid, centered on the optical nucleus, with spacings of 2′ in declination and 8 seconds (= 1.′67) in right ascension. A montage of the reduced spectra is shown in Figure 2. Table 3 lists basic profile parameters.

Column (1) of Table 3 gives the location of the beam center in minutes of arc with respect to the optical center of the galaxy. The letter-number code in the table refers to the coded positions in Figure 2. For convenience, positions are coded by R.A. and decl. and a letter-number code in column 2; e.g., position 4N1.7W = C6.

Column (3) is the integrated 21 cm line flux I_{21} in Jy km s^{-1}. The realistic uncertainty in these values is about 0.9 Jy km s^{-1}.

Column (4) is the velocity V_{50} of each profile (heliocentric), measured at the point where the flux drops to 50% of its peak value. The mean error (shown in

[3]Actually, the signal was divided, fed to two separate banks of 252 channels each, and then recombined to reduce the digitizing noise from the autocorrelator. The improvement in sensitivity is about 10%.

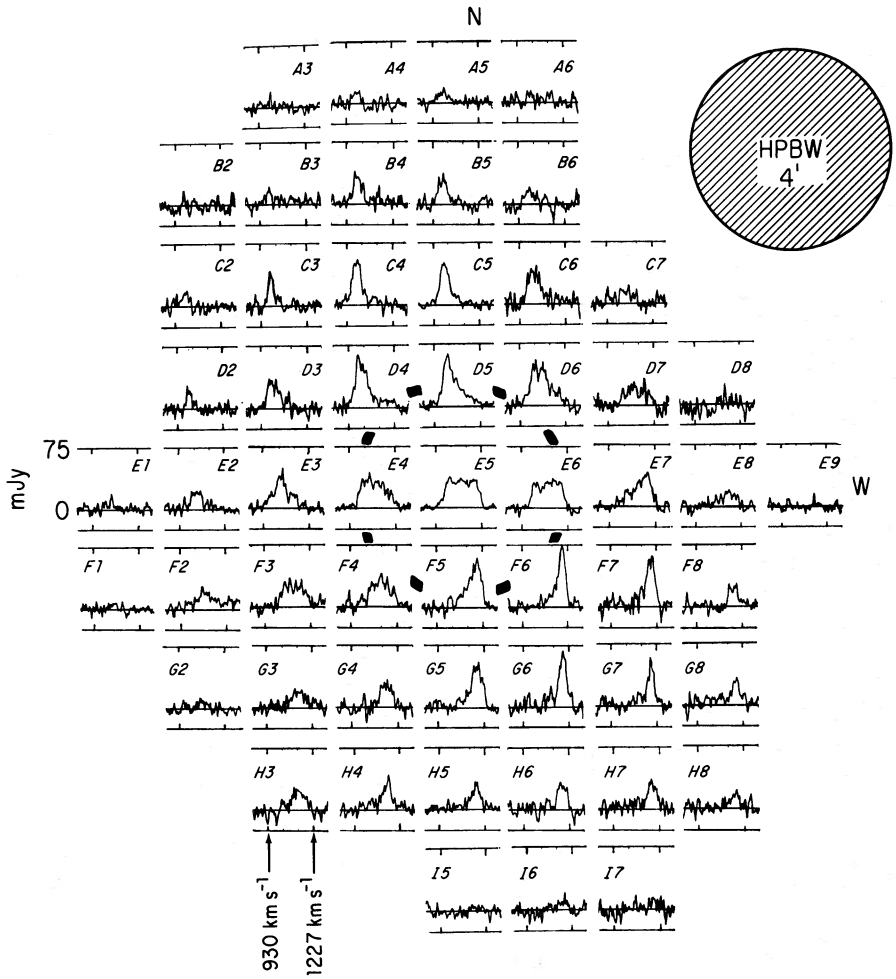

FIG. 2.—A montage of the 55 Arecibo spectra obtained for NGC 4203. North is up; west on the right. Grid positions are spaced 2′ in declination and 1.67′ in right ascension. Letter-number position code (e.g., E5) corresponds to code in Table 3. The hatched circle indicates the optical size of the galaxy.

parentheses) is taken to be one-half the difference between the 20% and 80% points. In general, we have attempted to measure V_{50} only for profiles stronger than 2 Jy km s^{-1}.

Column (5) is the velocity of the profile peak V_p. It is derived by fitting a Gaussian to the entire profile (or just to the spectral points higher than one-half the peak flux in asymmetric profiles, if marked with an asterisk).

Column (6) is the one-dimensional dispersion line width $V_{\rm disp}$ derived in the Gaussian fit for V_p. The line width is often dominated by different projected rotation velocities and is not necessarily indicative of the local random velocities.

III. GAS DISTRIBUTION AND KINEMATICS

a) The Velocity Field

An H I velocity contour map for the gas in NGC 4203 is given in Figure 3, derived from the V_p values in Table 3. No correction for beam smearing has been attempted. The dashed isovelocity contours are in regions where the velocity field is either unresolved or is ill-defined and serve to smoothly connect the outer isovelocity contours. The velocity field for the H I gas outside of the optical image is typical of that for a rotating disk (cf. Roberts 1975). However, the overall velocity field for the galaxy is somewhat distorted: the outermost NE-SW velocity contours are at an angle of about 40° to the center of the galaxy, while the innermost contours are at angles between 30° and 40°. The relative positions of the outermost velocity contours also suggest the presence of an S shaped distortion of the velocity field, albeit on a size scale near the spatial resolution of the present observations.

Since the velocity field is roughly symmetric about the center of the galaxy, one can use the profiles on opposite sides of the nucleus to estimate the center of mass velocity, $V_{\rm com}$ of the system as a whole. From 10 such

TABLE 3

PROFILE PARAMETERS FOR NGC 4203

Profile Position (1)	Position Code (2)	I_{21} (Jy km s^{-1}) (3)	V_{50} (km s^{-1}) (4)	V_p (km s^{-1}) (5)	(V_{disp}) (km s^{-1}) (6)
8N1.7W ...	A6	1.1	...	...	...
8N	A5	1.2	...	...	...
8N1.7E	A4	0.3	...	...	...
6N1.7W ...	B6	0.7	...	...	...
6N	B5	2.1	961 (10)	991 (2)	29 (2)
6N1.7E	B4	3.3	967 (5)	995 (2)	28 (2)
6N3.3E	B3	1.7	...	...	...
6N5E	B2	−0.6	...	...	...
4N3.3W ...	C7	2.1	...	...	...
4N1.7W ...	C6	4.4	967 (5)	1019 (2)	39 (2)
4N	C5	4.1	969 (17)	1002 (1)	32 (1)
4N1.7E	C4	4.3	957 (10)	992 (1)	29 (1)
4N3.3E	C3	1.5	967 (12)	987 (1)	16 (1)
4N5E	C2	0.9	...	...	...
2N5W.....	D8	−0.8	...	...	...
2N3.3W ...	D7	2.5	1016 (36)	1102 (7)	74 (7)
2N1.7W ...	D6	7.0	996 (27)	1054 (2)	64 (2)
2N	D5	6.7	981 (20)	1012 (1)[a]	41 (2)
2N1.7E	D4	6.3	971 (17)	1007 (1)	42 (1)
2N3.3E	D3	2.9	965 (16)	1005 (3)	41 (3)
2N5E	D2	1.8	971 (7)	1012 (2)	34 (2)
6.7W	E9	−0.3	...	...	...
5W	E8	1.7	...	...	...
3.3W	E7	4.7	1206 (18)	1169 (2)[a]	29 (2)
1.7W	E6	6.5	1212 (21)	...	...
Center.....	E5	7.3	981 (24) 1214 (18)	... ...	... ...
1.7E.....	E4	6.7	994 (21)	...	...
3.3E.....	E3	4.7	1008 (38)	1041 (2)	56 (2)
5E	E2	2.3	955 (25)	1038 (3)	44 (3)
6.7E.....	E1	0.8	...	...	...
2S5W	F8	2.0	1194 (23)	1164 (3)	32 (3)
2S3.3W	F7	4.7	1210 (16)	1181 (2)	32 (2)
2S1.7W	F6	5.4	1212 (10)	1186 (1)[a]	23 (1)[a]
2S	F5	5.9	1225 (18)	1181 (2)[a]	40 (2)[a]
2S1.7E	F4	5.5	1206 (33)	1119 (4)	71 (4)
2S3.3E	F3	4.3	1196 (25)	1107 (6)	89 (7)
2S5E	F2	3.8	...	...	...
2S6.7E	F1	0.2	...	...	...
4S5W	G8	1.4	1208 (5)	1173 (1)	26 (1)
4S3.3W	G7	3.3	1208 (16)	1185 (1)	20 (1)
4S1.7W	G6	5.1	1210 (15)	1183 (1)	24 (1)
4S	G5	5.0	1220 (19)	1174 (1)	39 (1)
4S1.7E	G4	1.9	1183 (21)	1146 (3)	37 (2)
4S3.3E	G3	2.4	1227 (52)	1134 (5)	58 (5)
4S5E	G2	0.4	...	...	...
6S5W	H8	1.5	...	...	...
6S3.3W	H7	3.2	1206 (23)	1173 (2)	27 (2)
6S1.7W	H6	2.4	1214 (16)	1177 (2)	27 (2)
6S	H5	2.7	1190 (42)	1162 (2)	30 (2)
6S1.7E	H4	3.3	1163 (19)	1139 (2)	29 (2)
6S3.3E	H3	1.8	...	...	...
8S3.3W	I7	0.6	...	...	...
8S1.7W	I6	0.0	...	...	...
8S	I5	−0.2	...	...	...

NOTE.—Errors in parentheses.

[a]Highly asymmetrical profiles; Gaussian fit made only to channels stronger than half of peak flux.

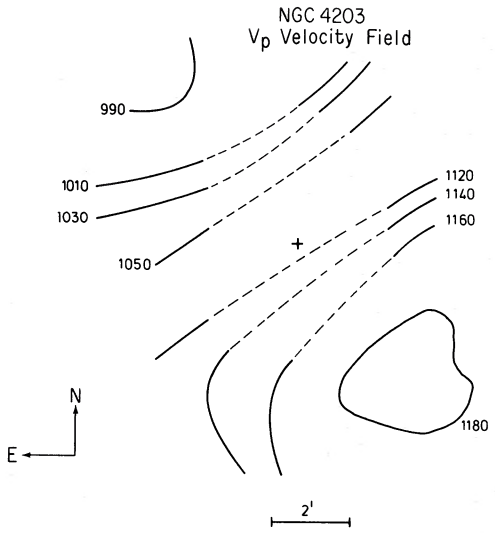

FIG. 3.—The velocity field for the H I disk of NGC 4203. The velocity values V_p are plotted, and a cross marks the optical center of the galaxy. The dashed lines are in regions where the velocity field is unresolved or ill-defined and serve to connect smoothly the outer isovelocity contours on either side of the galaxy. Regions with V_p velocities from 1050 to 1120 km s^{-1} are unresolved by these data (Table 3).

pairs with measured values of V_p, one derives $V_{com} = 1089 \pm 3$ km s^{-1}. From 12 such pairs with measured values of V_{50}, one obtains $V_{com} = 1094 \pm 3$ km s^{-1}. We adopt $V_{com} = 1091 \pm 3$ km s^{-1}. (This is also in good agreement with the mean radial velocity of 1097 km s^{-1} for the center profile).

An H I rotation curve can be derived directly from profiles at the positions C3, D4, F6, and G7, which lie along P.A. = 35°, and from the center profile. The H I disk of NGC 4203 is of comparable size to the Arecibo beam, so that V_{50} is to be preferred for the rotation curve over V_p. This is because V_{50} better approximates the true rotation velocity along the major axis as measured from a global profile (Krumm and Salpeter 1979*a*).

The H I rotation curve derived from these data is shown in Figure 4, where the values of V_{50} from the center profile are plotted beyond 2′, corresponding to one-half the beamwidth. Also plotted in Figure 4 is the rotation curve interior to 0.′25 derived from the Hα and Ne II emission lines, as observed and measured by V. C. Rubin, who has kindly permitted us to publish these data. The optical rotation curve is centered about the radial velocity determined by Rubin for NGC 4203, 1075 ± 10 km s^{-1}, which is 75 km s^{-1} higher than the velocity quoted in the RC2, and not significantly different from the value for V_{com}. Due to uncertainties in relative position angles for these rotation curves (see below), the optical and radio rotation curves are plotted as observed.

Within the errors, the H I rotation curve for NGC 4203 is flat beyond 2′ and can be traced to at least 4′ ($= 12.3\ h^{-1}$ kpc). The average projected value of the rotation velocity is $V_r \sin i = 120 \pm 5$ km s^{-1}. On the other hand, the relatively high optical velocities observed close to the nucleus, combined with the shapes of the H I velocity profiles near the center of the galaxy, indicate that the gas distribution/velocity field of NGC 4203 is complex inside a radius of 1′: the spectroscopic data of Rubin show that the rotation velocity inside 15″ is relatively constant at 155 km s^{-1}, reaching this velocity within 3″ ($= 150\ h^{-1}$ pc). This is significantly higher than the value of 120 km s^{-1} in the outer parts of the galaxy, even though the optical rotation curve was obtained at a P.A. = 10° (corresponding to the P.A. of the optical axis; Burstein 1979*b*).

Furthermore, the H I center is flat-topped and shows no appreciable H I gas at velocities greater than ± 120 km s^{-1}. If the flat rotation curve that is defined outside of 2′ extended into the center and smoothly joined to a Keplerian falloff from the inner velocity curve, one would expect that velocity crowding would produce a "double-horned" central profile (providing the H I distribution were centrally condensed). The horns could be suppressed if the observed rotation curve were solid-body inside of 2′, or if the H I disk were viewed very edge-on (cf. the central profile for the edge-on spiral NGC 4565 in Krumm and Salpeter 1979*b*). The first possibility appears excluded by the higher central velocity in the galaxy, while the second possibility requires an inclination of 70° or more to the line of sight, very different from the optical inclination of about 25°.

A distortion of the outer velocity field, a probably complicated inner velocity field and/or H I distribution, and major asymmetries in the outer H I distribution (§ III*c*) are phenomena that are commonly observed in the H I disks of spiral galaxies (Bosma 1978) as well as in the H I disk of NGC 4203. Spiral galaxies with near neighbors often show large-scale asymmetries in their velocity fields, while S shaped distortions of velocity fields are commonly seen in spirals and can be the

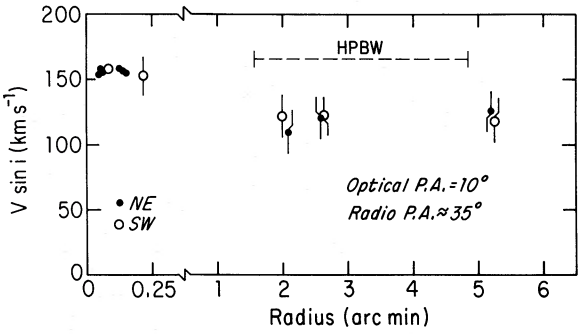

FIG. 4.—The major axis rotation curve as derived from the H I data (outer scale) at a position angle of 35°, and from the optical data of Rubin (inner scale) at a P.A. = 10°. The profile edge, V_{50} is plotted for the 21 cm H I data, and the dashed line indicates the H I beamwidth.

product of an oval distortion in a coplanar disk or of a real warping of the plane (Bosma 1978). As analyzed by Bosma, most galaxies with oval distortions have a continuously changing P.A. of the kinematic major axis within the optical image of the galaxy, and the H I and optical luminosity distributions are of similar size. Galaxies with warped H I disks (termed a kinematical warp when seen as an S shaped distortion of the velocity field; cf. Sancisi 1977 for direct observations of warps) usually have H I disks that extend well beyond the optical image, but have a coincidence of the kinematical and the optical major axes within the optical image.

The relative H I and optical distributions and the velocity field in NGC 4203 share several characteristics in common both with spiral galaxies having oval distortions and with spirals having kinematical warps, but NGC 4203 has no near neighbor with which to interact (§ IV). The present data are at once of both too fine and too coarse a resolution to choose among the various possibilities but are most consistent with the distortions in the velocity field in NGC 4203 being the product of an oval distortion in the H I disk, or, alternatively, of a warping of the plane of the disk.

b) *The Velocity Dispersion in the* H I *Disk*

While the distribution of H I gas in the inner part of the galaxy is not clear from these data, the H I gas outside the optical disk of the galaxy is distributed in a rotating disk. An estimate of the relative thickness of this disk can be made by comparing the circular velocity to the average velocity dispersion perpendicular to the disk. In general, the line widths, $V_{\rm disp}$ given in Table 3 are contaminated by projected rotation across the beam. The line widths accurately measure the local noncircular velocities only in the limit of large radii and/or a face-on disk.

Although the beam of the telescope is of comparable angular size to the H I disk, inspection of Figure 3 shows that the effect of differential rotation across the beam is minimal for positions at large radial distance along the major axis. Indeed, the narrowest of the profiles in Figure 2 are found at positions straddling the major axis.

Four of the narrowest profiles in Figure 2, C4, C3, G6, and G7 are of sufficient signal-to-noise ratio to measure $V_{\rm disp}$ reliably. Two other positions with lower signal-to-noise ratio profiles, D2 and G8, were reobserved with a channel spacing of 2 km s^{-1} to obtain a better measure of $V_{\rm disp}$. The reobserved velocity values are given for these two positions in Table 3. The mean value of $V_{\rm disp}$ for the five narrowest profiles is 23 ± 5 km s^{-1}. From the discussion above, this value of $V_{\rm disp}$ can only be an upper limit to the perpendicular velocity dispersion in the disk. Thus the ratio $V_r/V_{\rm disp} \geq 6 \csc i$, where i is the inclination of the galaxy to the plane of the sky ($i=0°$ for face-on). One concludes that the H I disk in NGC 4203 is relatively thin.

On the other hand, the average value of 23 km s^{-1} for $V_{\rm disp}$ measured in this manner is significantly higher than the velocity dispersion of H I gas in our own Galaxy, about 5 km s^{-1} (e.g., Crovisier 1978). It is unlikely that the higher value of $V_{\rm disp}$ in NGC 4203 is due only to differential rotation across the beam, since the velocity fields at positions G8 and C3 indicate essentially no differential rotation contributing to these profiles. Furthermore most of the individual velocity profiles in Figure 2 are more slope-sided than those of the H I disks of spirals taken at comparable resolution (cf. Krumm and Salpeter 1979*a*). As further evidence, the global H I profile for NGC 4203, obtained by adding the profiles from all 55 positions, is given in Figure 5 (cf. the global profile obtained by Knapp *et al.* 1977). The sides of the global profile are also slope-sided and resemble the flat rotation curve model profile of Roberts (1978) with a velocity dispersion of 20 km s^{-1}.

While not conclusive, the available data certainly suggest that the velocity dispersion of the gas in the disk of NGC 4203 is larger than that of the gas in a comparably-sized spiral galaxy. However, this result needs to be verified by higher resolution data.

c) *The* H I *Distribution*

A deconvolved map of the H I distribution in NGC 4203 was generated in the following manner: the flux integral distribution, as determined from the individual profiles was Fourier transformed and divided by the Fourier transform of the beam shape (assumed Gaussian), and the quotient was then transformed back. A filter was applied to the data in the transform domain to reduce the noise level in the deconvolved map.

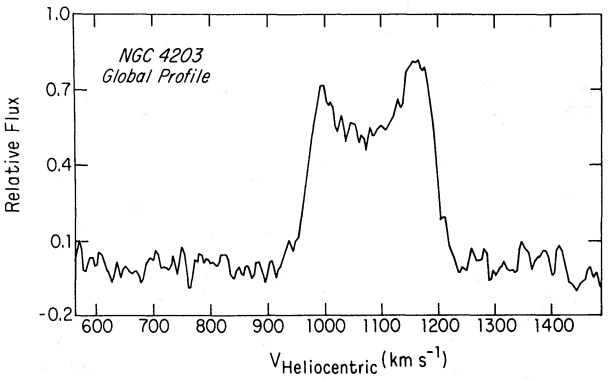

FIG. 5.—The global profile for the H I distribution in NGC 4203, obtained by summing all 55 observed positions. The vertical flux scale has an arbitrary normalization (cf. the profile of Knapp *et al.* 1977). Note the sloping sides to the profile, similar to those produced by a model disk with a flat rotation curve and a disk velocity dispersion of 20 km s^{-1} (Roberts 1978).

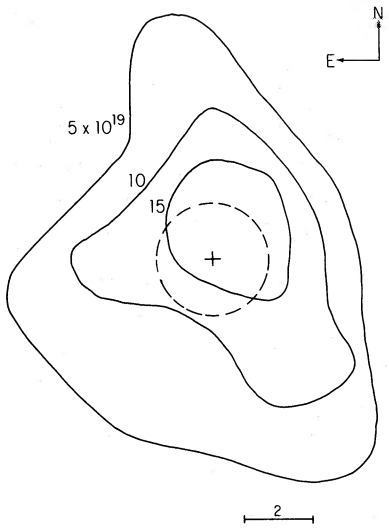

FIG. 6.—The deconvolved H I distribution in NGC 4203 at a resolution of 4′. Solid lines are contours at 5, 10, and 15×10^{19} cm^{-2}, and the dotted line indicates the optical extent of the galaxy. Although not resolved at this scale, the center profile indicates that the gas distribution has a minimum at the center.

As a result, H I features of intrinsic size less than about 4′ (FWHM) are smoothed out, and only the broad features of the distribution can be seen in the resulting column density map, shown in Figure 6. The outermost contour, at 5×10^{19} cm^{-2}, is at a level of three times the rms uncertainty (0.9 Jy km s^{-1}) and is at a diameter of $12\pm2'$, or 38 h^{-1} kpc. In comparison, the blue optical diameter at 26.5 mag arcsec^{-2} (the Holmberg radius) is only 4.2 (Burstein 1979*b*). Thus, the present data indicate that *the* H I *disk in NGC 4203 is at least three times the optical size of the galaxy*. Such a large ratio of H I to optical diameters has hitherto been found only in a few spirals, mostly of late types (Bosma 1978; Huchtmeier, Serradakis, and Materne 1980; Hawarden *et al.* 1979).

Despite the relative size of the H I disk, the total amount of hydrogen gas in the galaxy is not very large. The integrated mass of H I derived from Figure 6 is

$$M_{\rm H\,I}=7.5\pm0.3\times10^{8}\,h^{-2}\,M_{\odot},$$

in good agreement with the value of $5.5\times10^{8}\,h^{-2}\,M_{\odot}$ obtained by Knapp *et al.* (1977), when it is considered that the H I disk is comparable in size to their 20′ beam. The distance-independent ratio of $M_{\rm H\,I}/L_B$ is 0.17 ± 0.01, typical of early-type spirals, but over an order of magnitude larger than the upper limits of 0.01 that can be set on the majority of S0 galaxies (e.g. Bieging and Biermann 1977).

The deconvolved H I distribution is asymmetric, with its centroid shifted about 3′ west of the optical nucleus of the galaxy. The outermost contour in Figure 6 is at three times the rms noise in the fluxes, so that much of the asymmetry is probably real. A further inference about the gas distribution in NGC 4203 can be made by noting that the flux integral for the center position is not significantly higher than those of the four adjacent positions. Such a situation can occur only if there is a relative decrease in H I density interior to the 2″ radius defined by the central beam. Thus, these data suggest that the H I gas density decreases within the optical disk of the galaxy. Again, a higher resolution map would be desirable to confirm the existence of a central minimum.

It is useful to make an azimuthally-averaged parametrization of the H I disk in NGC 4203 in order to compare this disk to those found in spiral galaxies. As in Krumm and Salpeter (1979*b*) a model is assumed in which the column density of H I is a Gaussian function of the radius r:

$$N_{\rm H\,I}(r)=N_0\exp\left[-\left(r^2/r_{\rm H\,I}^2\right)\right]. \qquad (1)$$

The specification of the angle of inclination, i, and the position angle of the major axis, P.A., serve to orient the model on the plane of the sky. The P.A. was constrained to be 35°, consistent with Figures 3 and 6, so that there are three independent parameters (N_0, the central H I gas surface density; $r_{\rm H\,I}$, the Gaussian width of the H I; and i). Models were constructed for discrete intervals in a range of values for these three parameters and convolved with the telescope beam. These models were then compared to the observed fluxes listed in Table 3, and the best fit (in a least-squares sense) was found. This procedure yields

$$N_0=1.4\pm0.4\times10^{20}\ {\rm cm}^{-2},$$

$$r_{\rm H\,I}=3.5'\pm0.6',$$

and

$$i=42°\pm15°,$$

where the errors correspond to an increase of χ^2 by a factor of 2 over the minimum. N_0 is normalized so that the total flux from the model galaxy equals the total observed flux.

The large value of $r_{\rm H\,I}$ reflects the lack of a strong gradient in the gas distribution, and the large error in i reflects the outer asymmetry of the disk. The average central density N_0 is relatively well determined and can be compared to that of spirals. NGC 925 is an SBc galaxy of similar intrinsic size and luminosity as NGC 4203 and has been measured in an analogous manner by Krumm and Salpeter (1979*b*) to have $N_0=2\times10^{21}$ cm^{-2}. The average gas column density perpendicular to the disk in our own Galaxy is $0.5\text{–}2\times10^{21}$ cm^{-2} at the solar radius (Heiles 1976), so that the gas column density in NGC 4203 is an order of magnitude less than in these spirals (see also § IV).

With the additional possibility that the gaseous disk of NGC 4203 is thicker than those of its spiral counterparts, it is clear that the average space density of gas in the disk of NGC 4203 is very much less than the gas density in comparably sized disks of spiral galaxies. This lower gas density in NGC 4203 has obvious implications for the star formation history of its disk, some of which will be explored in § IV.

d) *The Inclination of the Galaxy*

As mentioned in the Introduction, the optical appearance of NGC 4203 on typical classification plates is symmetric and smooth, and the overall luminosity distribution in the galaxy is exponential, indicating that most of the stars are in a disk. The apparent orientation of the galaxy within the 24th mag arcsec^{-2} isophote can be determined from the surface photometry of Burstein (1979*b*; a bright nearby star confuses the fainter isophotes). The optical position angle is $8° \pm 1°$, in good agreement with the value of 10° given by Nilson (1973); and the axial ratio is 0.89 ± 0.04, implying $i = 27° \pm 5°$ for a circular disk.

Although the derived H I and optical inclinations are not significantly different (only a one sigma difference), the kinematical position angle derived from the H I velocity field is at least 25° different from the position angle of the optical disk. The difference in P.A. between the inner optical disk and the outer H I disk is probably real and is also found in spiral galaxies with oval distortions or kinematical warps (Bosma 1978).

Using an average value for the inclination $i = 35° \pm 7°$, and P.A. $= 35°$, $V_{max} = 210 \pm 40$ km s^{-1} for NGC 4203, where the uncertainty in V_{max} is primarily due to the uncertainty in the angle of inclination of the H I disk.

e) *The Mass Distribution in NGC* 4203

If the mass distribution in NGC 4203 is spherically symmetric, the mass interior to a radius in $M(r) = 2.327 \times 10^5 \; V^2 r M_\odot$, where V is the circular velocity in km s^{-1} and r is in kpc. The integrated mass of a disklike distribution is smaller by only a few percent (cf. Rubin, Ford, and Thonnard 1978). At the Holmberg radius of $r = 2'.1$ or $6.7\ h^{-1}$ kpc, the mass of NGC 4203 is $6.8 \pm 10^{10}\ h^{-1}\ M_\odot$. The total mass interior to the furthest reliably measured radius, 5′ ($16\ h^{-1}$ kpc) is $1.6 \times 10^{11}\ h^{-1}\ M_\odot$. The ratio of total neutral hydrogen mass to the gravitational mass interior to the Holmberg radius is about $0.01\ h^{-1}$, or an order of magnitude smaller than in a typical spiral galaxy (Roberts 1975).

The mass-to-light ratio of NGC 4203 interior to the Holmberg radius, $(M/L)_{Holm}$, is $15 \pm 5\ h$. This value of $(M/L)_{Holm}$ is quite comparable to that obtained by Faber and Gallagher (1979) for early-type spirals (taking into account the differences in H_0). However, the total observable mass of NGC 4203 leads to a value of $(M/L)_{obs} = 35 \pm 12\ h$, since the H I gas traces out the rotation curve well outside the Holmberg radius. Table 4 summarizes the properties of the H I disk and the mass distribution in NGC 4203 derived from the H I data.

A flat rotation curve implies that the radial mass surface density, σ_M, is proportional to r^{-1}. The azimuthally averaged H I surface density distribution in NGC 4203, $\sigma_{H\,I}$, is also approximately proportional to r^{-1}, as given by the model in § III*c*. Thus the ratio $\sigma_M/\sigma_{H\,I}$ is nearly independent of radius for the gaseous disk of NGC 4203, at least exterior to the optical disk of the galaxy, and equal to about 600. A constant value of the ratio $\sigma_M/\sigma_{H\,I}$ has previously been found for some spiral galaxies (Bosma 1978, Fig. 7, p. 169). Bosma shows that while the absolute value of $\sigma_M/\sigma_{H\,I}$ does vary, most of the spirals in his study reach a constant value of $\sigma_M/\sigma_{H\,I}$ in their outer disks. In some of the spiral galaxies with extended H I disks, $\sigma_M/\sigma_{H\,I}$ is constant over three-quarters of the disk.

In contrast, it is well known (e.g., Bosma and van der Kruit 1978) that exponential stellar disks, such as observed in NGC 4203 and in most spirals, combined with flat rotation curves, require that the ratio of σ_M to the luminosity surface density increase radially outwards. Therefore, the present analysis indicates that the mass, luminosity, and H I structures in NGC 4203 are remarkably similar to those observed in spiral galaxies.

The flat rotation curves observed both in spirals and in NGC 4203 imply that most of the mass in these galaxies is in nonluminous form. In the case of NGC 4203, at least twice as much mass lies exterior to the Holmberg radius as lies interior to it. Furthermore, the constancy of $\sigma_M/\sigma_{H\,I}$ in the outer disks of both spirals and NGC 4203 suggests that the extended H I disks of these galaxies are closely associated with this nonluminous mass component.

TABLE 4

THE H I DISK OF NGC 4203

Position angle	$35° \pm 5°$
$V \sin i$	120 ± 5 km s^{-1}
V_{com}	1091 ± 3 km s^{-1}
V_{disp}	23 ± 5 km s^{-1}
H I diameter at 5×10^{19} cm^{-2}	$12' \pm 2' = 38 \pm 6\ h^{-1}$ kpc
$M_{H\,I}$	$7.5 \pm 0.3 \times 10^8\ h^{-2}\ M_\odot$
$M_{H\,I}/L_B$	$0.17 \pm 0.01\ M_\odot/L_\odot$
N_0	$1.4 \pm 0.4 \times 10^{20}$ cm^{-2}
$r_{H\,I}$	$3'.5 \pm 0'.6 = 22.0 \pm 1.9$ kpc
Inclination, i:	
Observed	$40° \pm 10°$
Assumed	$35° \pm 7°$
$V_{rotation}$	210 ± 40 km s^{-1}
$M_{GAL}(R_{Holm})$	$6.8 \pm 2.3 \times 10^{10}\ h^{-1}\ M_\odot$
$M_{H\,I}/M_{GAL}(R_{Holm})$	$0.011 \pm 0.003\ h^{-1}$
$M_{GAL}/L_B(R_{Holm})$	$15 \pm 5\ h\ M_\odot/L_\odot$
M_{GAL}/L_B (obs)	$35 \pm 12\ h\ M_\odot/L_\odot$

IV. COMPARISON OF NGC 4203 WITH OTHER GALAXIES

The present observations indicate that the distributions of mass, luminosity, and H I gas in NGC 4203 are remarkably similar to those found in spiral galaxies, especially those spirals with extended H I disks. As an example, compare NGC 4203 with a classical Sb galaxy, NGC 2841 (Sandage 1961). As summarized by Bosma (1978), NGC 2841 has: (1) an H I disk at least 2.5 times the Holmberg radius; (2) an asymmetric, warped gas distribution with a central minimum; (3) a flat rotation curve; (4) a kinematical warp such that the P.A. of the outer velocity contours is at a significant angle to the major axis of the optical distribution; and (5) a constant ratio of $\alpha_M/\sigma_{\rm H\,I}$ in the outer 70% of the H I disk. While NGC 2841 is somewhat larger than NGC 4203, both galaxies have disk-to-bulge ratios of about 2 (cf. Boroson 1981 for NGC 2841).

Comparisons with galaxies on the other end of the Hubble sequence are limited since detailed investigations of the gas distributions in only two other H I-rich early-type galaxies have been published. The H I distribution/velocity field in NGC 1023, an edge-on S0, is complex and not easily interpretable (Hart, Davies, and Johnson 1980).

On the other hand, the H I distribution and velocity field in the elliptical galaxy NGC 4278, as observed by Raimond *et al.* (1981) at Westerbork, is again remarkably similar to that observed in NGC 4203. As discussed by Raimond *et al.* (1981), NGC 4278 has: (1) an H I ring, with a central minimum and extent nearly twice the optical size of the galaxy; (2) an asymmetric gas distribution; (3) an approximately flat rotation curve; and (4) a position angle of the outer velocity contours of the H I gas that is at a significant angle to the optical major axis. Further inspection of their data convolved to 3′ (roughly our resolution) indicates that: (5) $\sigma_M/\sigma_{\rm H\,I}$ in the ring is on the order of 200 (assuming $i=45°$ and adjusting to $H_0=100$ Mpc km s^{-1}); and (6) the maximum smoothed H I column density is about 10^{20} cm^{-2}.

If NGC 4203, 4278, and 2841 have H I distributions and velocity fields so similar in structure, why then is one classified an S0, one an elliptical, and one an Sb? Some of the differences in morphological appearance are undoubtedly connected with one significant difference among the galaxies: the average gas surface density in the disk of NGC 4203 and in the "ring" of NGC 4278 is almost an order of magnitude lower than in the disk of NGC 2841. A higher velocity dispersion in the H I disk of NGC 4203 than in the H I disk of NGC 2841 would make the difference in volume gas densities between these two disks even greater.

Although no direct evidence links low star formation rates with low gas densities, it is reasonable to associate the lack of obvious star formation in NGC 4203 and NGC 4278 with the very low gas densities in these galaxies. This association is especially valid if star formation requires a threshold or minimum value of gas density to proceed efficiently. The extent of star formation that is occurring in the gaseous disk of NGC 4203 is consistent with this view, since it is of such low surface brightness as to require exceptionally deep ultraviolet plates to detect it (§ I).

The only morphological difference between NGC 4203 and NGC 4278 is that the former has a readily visible stellar disk. However, the presence of a stellar disk in NGC 4278 cannot be ruled out from presently available data, since disks that contribute much less than 50% of the luminosity of the bulge are difficult to detect (Burstein 1979*c*).

NGC 2841 and NGC 4203 share another common characteristic—both are relatively isolated in space (see Bosma 1978 for NGC 2841). The nearest comparably sized galaxy to NGC 4203 is many galaxy diameters away (Zwicky and Herzog 1966). As pointed out by Bosma (cf. Sancisi 1977), NGC 2841 is one of several isolated spiral galaxies with asymmetric, warped H I disks, although few have as extended a disk. Approximately 30% of the sample of spirals studied by Bosma showed evidence of warped disks. The origin and persistence of the warps and asymmetries in the disks of the isolated spirals is as yet unknown, since no obvious tidal companion is present (Bosma 1978; see also Tubbs and Sanders 1979).

V. SPECULATIONS ON THE ORIGIN OF H I GAS IN EARLY-TYPE GALAXIES

The absence of observable H I gas in most ellipticals and S0's is now usually ascribed to the efficiency of a self-cleaning mechanism that disperses the gas ejected from evolving stars (e.g., Faber and Gallagher 1976; Knapp, Kerr, and Williams 1978). As long as the number of early-type systems with detected H I was small, a tidal capture model for the origin of the gas was attractive (e.g., Knapp, Kerr, and Williams 1978). In this model, the gas distributions in ellipticals and some S0's are the result of the tidal capture of H I gas that was originally associated with spiral galaxies. Apparent examples of tidal-capture processes are found in such elliptical-spiral pairs as NGC 4627–4631 (Weliachew, Sancisi, and Guelin 1978) and NGC 1510–1512 (Disney and Pottasch 1977; Hawarden *et al.* 1979). In both cases, the elliptical in the interaction is relatively small and its integrated starlight is dominated by a young stellar component (Burstein 1979*a*; Disney and Pottasch 1977).

However, the number of red, old stellar population ellipticals and S0's with detected H I has grown substantially over the last several years (Gouguenheim 1979; Krumm and Salpeter 1979*c*). The sheer number of detections, combined with the isolation of galaxies like

NGC 4203, has served to diminish the viability of the tidal capture model for the origin of H I gas in all H I-detected ellipticals and S0's. Even so, a tidal capture model for the H I gas in any particular early-type galaxy cannot be *a priori* ruled out (cf. the discussion of Raimond *et al.* [1981] for NGC 4278), especially when possible spiral galaxy donors are present.

On the other hand, the marked similarities brought out by the comparison of the previous section strongly indicate that the formation histories of the gas distributions in NGC 4203 and NGC 4278 were similar to those of spirals with extended H I disks. Since the gaseous disks of these spirals are assumed to be intrinsically associated with their optical counterparts, one is led to the inference that *the gas distributions in NGC 4203 and probably in NGC 4278 are intrinsically associated with their optical components*. The term "intrinsically associated" is intentionally vague, as it is not at all clear how such extended H I disks are formed; nor is it clear why the gas distributions in these disks are usually strongly asymmetric, even in apparently isolated galaxies (cf. discussion in Bosma 1978).

If more of the optically-normal ellipticals and S0's with H I gas are found to have extended H I disks like those in some spiral galaxies, then the further implication that *many* ellipticals and S0's originally had H I disks must be seriously considered. The present data are highly suggestive; further detailed H I *and* optical data on H I-rich red ellipticals and S0's are necessary to discover if the morphology and kinematics of an extended, asymmetric H I disk are ubiquitous among early-type galaxies with H I.

We are grateful for the use of the Arecibo telescope and the help of the staff of NAIC, which is operated by Cornell University under contract with the National Science Foundation. Discussions with George Miley, Colin Norman, Ed Salpeter, Jay Gallagher, Allan Tubbs, and Vera Rubin were especially useful. N. K. acknowledges the support of the Netherlands Foundation for Pure Scientific Research (Z.W.O.) during the last stages of this work; and D. B., the support of the Department of Terrestrial Magnetism, Carnegie Institution of Washington, during the initial stages of this work.

REFERENCES

Allen, C. W. 1973, *Astrophysical Quantities*, 3rd ed. (London: Oxford University Press).
Balick, B., Faber, S. M., and Gallagher, J. S. 1976, *Ap. J.*, **209**, 710.
Bieging, J. H., and Biermann, P. 1977, *Astr. Ap.*, **60**, 361.
Boroson, T. 1981, *Ap. J.*, in press.
Bosma, A. 1978, Ph.D. thesis, University of Groningen, The Netherlands.
Bosma, A., and van der Kruit, P. C. 1979, *Astr. Ap.* **79**, 281.
Bridle, A., Davis, M., Fomalont, E., and Lequeux, J. 1972, *A.J.*, **77**, 405.
Burstein, D. 1979*a*, *Ap. J.*, **232**, 74.
_____. 1979*b*, *Ap. J. Suppl.*, **41**, 435.
_____. 1979*c*, *Ap. J.*, **234**, 435.
Burstein, D., and Heiles, C. 1978, *Ap. J.*, **225**, 40.
Crovisier, J. 1978, *Astr. Ap.*, **70**, 43.
de Vaucouleurs, G., de Vaucouleurs, A., and Corwin, H. G., Jr. 1976, *Second Reference Catalogue of Bright Galaxies* (Austin: University of Texas Press) (RC2).
Disney, M. J., and Pottasch, S. R. 1977, *Astr. Ap.*, **60**, 43.
Dressel, L. L., and Condon, J. J. 1978, *Ap. J. Suppl.*, **36**, 53.
Faber, S. M., and Gallagher, J. S. 1976, *Ap. J.*, **204**, 365.
_____. 1979, *Ann. Rev. Astr. Ap.*, **17**, 135.
Gouguenheim, L. 1979, in *Photometry, Kinematics and Dynamics of Galaxies*, ed. D. S. Evans (Austin: University of Texas), p. 201.
Hart, L., Davies, R., and Johnson, S. 1980, *M.N.R.A.S.*, **191**, 269.
Hawarden, T. G., van Woerden, H., Mebold, U., Goss, W. M., and Peterson, B. A. 1979, *Astr. Ap.*, **76**, 230.
Heiles, C. 1976, *Ap. J.*, **204**, 379.
Hodge, P. 1969, *Ap. J. Suppl.*, **18**, 73.
Hohlfeld, R. G., and Krumm, N. 1981, *Ap. J.*, **244**, 476.
Huchtmeier, W. K., Serradakis, J. H., and Materne, J. 1980, *Astr. Ap.*, **91**, 341.
Knapp, G. R., Gallagher, J. S., Faber, S. M., and Balick, B. 1977, *A.J.*, **82**, 106.
Knapp, G. R., Kerr, F. J., and Williams, B. A. 1978, *Ap. J.*, **222**, 800.
Krumm, N., and Salpeter, E. E. 1979*a*, *Ap. J.*, **227**, 776.
_____. 1979*b*, *A.J.*, **84**, 1138.
_____. 1979*c*, in *Photometry, Kinematics, and Dynamics of Galaxies*, ed. D. S. Evans (Austin: University of Texas Press), p. 209.
Krumm, N., and Sramek, R. 1981, in preparation.
Nilson, P. 1973, *Uppsala General Catalogue of Galaxies* (Uppsala: Uppsala).
Raimond, E., Faber, S. M., Gallagher, J. S., and Knapp, G. R. 1981, *Ap. J.*, in press.
Roberts, M. R. 1975, in *Stars and Stellar Systems IX: Galaxies and the Universe*, ed. A. Sandage, M. Sandage, and J. Kristian (Chicago: University of Chicago Press), p. 309.
_____. 1978, *A.J.*, **83**, 1026.
Rubin, V. C., Ford, W. K., Jr., and Thonnard, N. 1978, *Ap. J. (Letters)*, **225**, L107.
Sancisi, R. 1977, *Astr. Ap.*, **53**, 159.
Sandage, A. 1961, *The Hubble Atlas of Galaxies* (Washington: Carnegie Institution).
Shostak, G. S., van Woerden, H., and Schwarz, U. J. 1979, in *Photometry, Kinematics, and Dynamics of Galaxies*, ed. D. S. Evans (Austin: University of Texas Press), p. 213.
Tubbs, A. D., and Sanders, R. H. 1979, *Ap. J.*, **230**, 736.
Weliachew, L., Sancisi, R., and Guelin, M. 1978, *Astr. Ap.*, **65**, 37.
Zwicky, F., and Herzog, E. 1966, *Catalogue of Galaxies and Clusters of Galaxies*, **III** (Pasadena: California Institute of Technology).

DAVID BURSTEIN: National Radio Astronomy Observatory, Edgemont Road, Charlottesville, VA 22901

NATHAN KRUMM: Sterrewacht Leiden, Huygens Lab, Wassenaarseweg 78, Leiden 2405, The Netherlands

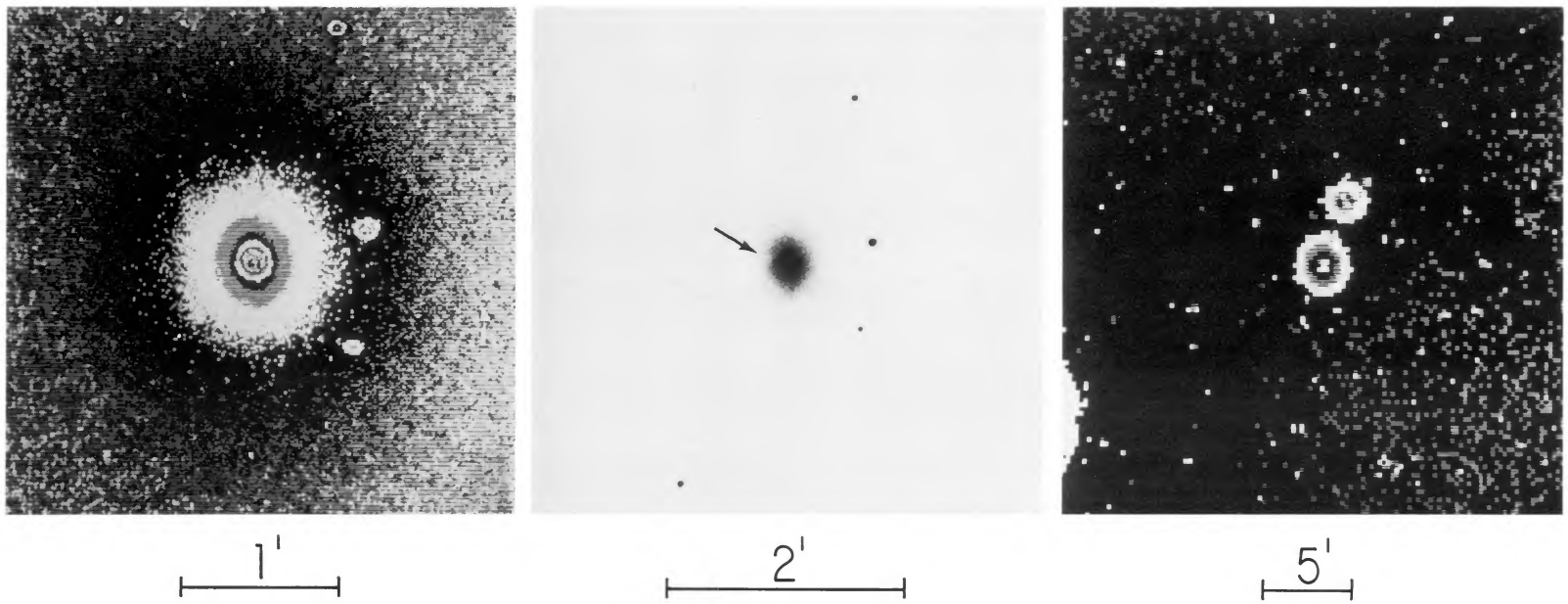

FIG. 1.—NGC 4203: Isophotal maps and a copy of a short exposure Crossley plate, all in the photographic *B* band. The left-hand isophotal map is from three Crossley plates, digitally summed, and is approximately 197″ on a side. The middle print is approximately 270″ on a side. The right-hand isophotal map is from two 1.2 m Palomar Schmidt plates, summed, and is 28.8′ on a side. North is up, and west to the right. An arrow points to an absorption feature in the luminosity distribution. See Burstein 1979*b* for details.

BURSTEIN AND KRUMM (*see* p. 518)